



# 3D printable inter cross-linking network (ICN) gels for reversible transparency control with water content

Yosuke Watanabe<sup>1</sup> · Shota Inoue<sup>1</sup> · Azusa Saito<sup>1</sup> · Masasu Kawakawami<sup>1</sup> · Hidemitsu Furukawa<sup>1</sup>

Received: 1 July 2019 / Accepted: 15 July 2019 / Published online: 19 July 2019  
© The Author(s) 2019

## Abstract

A patient-specific phantoms, which are equivalent to human tissues, is needed in the experimental dosimetric verification before radiotherapy treatments. Most of the shape of gel phantoms have been structurally limited because of the fabrication method using mold technique. The present study focuses on direct freeform fabrication of gel phantom with the customized optical 3D gel printing system. Life-sized gel phantoms were replicated using conventional mold techniques, the 3D printer with two-step sequential free-radical polymerization process and inter cross-linking network gels as 3D printing materials. The gel phantoms are ultraviolet light-sensitive instead of radiation. The ultraviolet sensitivity of the gel phantoms (using mold techniques) with different molar ratios were experimentally evaluated with transmittance measurements, and were theoretically estimated by curve fitting to the observed data. This measurement gave us the insight that more vinyl monomers in the gel phantoms caused rapid polymerization and visibly opaque as well as conventional gel dosimeters. We confirmed that inter cross-linking network gel was 3D printable with the customized 3D printer, with resolution of fabrication 500  $\mu\text{m}$ , as pre-finger-shaped phantom. The cross section of 3D printed gel phantom showed the distribution of opacity, that is, the distribution of UV irradiation. We expect that the 3D printer specialized gel materials and ICN gels are feasible for practical fabrication method of 3D gel phantom.

## 1 Introduction

Radiotherapy is one of standard treatments for cancer with fewer treatment-related side effects than chemotherapy and surgery (Etsuo 2017). In the radiotherapy treatments, suitable radiation should be delivered to the target volume as much as possible while less radiation should be directed at the normal cells that are nearby. The techniques, such as intensity-modulated radiation therapy (IMRT) and volumetric modulated arc therapy (VMAT) (Etsuo 2017; Wagter 2004; Yuichiro 2004; Yuichiro et al. 2002), for delivering radiation have recently been developed and the ultimate concentration of radiation have now been achieved with them. Especially, it is necessary to carry out the experimental dosimetric verification before radiotherapy treatments, and generally phantoms have been used for the verification because it is difficult to directly measure

actual 3D dose distribution at the target volume inside human body. Recent investigations have demonstrated that additive manufacturing enables us to fabricate the desired shape of phantoms (Takeshi et al. 2017; Forte et al. 2016; Elter et al. 2019; Pantelis et al. 2018; Leonard et al. 2018; Fabian et al. 2016). Due to the irradiated regions in polymer gels becoming visibly opaque with absorbed dose, polymer gels have been considered as an alternative to water as material of phantoms. However, few studies have focused on directly fabricating the 3D printed phantoms consisting of gel materials without using 3D printed mold. In comparison with molded counterparts, direct 3D printing offers the possibility of more freely printing 3D structures such as a hollow structure. In our previous work, 3D printed hollow objects made of gel materials were fabricated with a customized optical 3D printing system (Shiblee et al. 2019), and the 3D printed objects of multifunctional ionic gels incorporating ionic liquid (IL) in the thiol–ene network of thiol-based end-crosslinker and acrylate monomers were fabricated using commercial stereolithography (SLA) 3D printing system (Kumkum et al. 2018). It was found that optical 3D printing system

✉ Hidemitsu Furukawa  
furukawa@yz.yamagata-u.ac.jp

<sup>1</sup> Soft and Wet Matter Engineering Laboratory, Department of Mechanical Systems Engineering, Yamagata University, Yonezawa, Japan

utilized to fabricate gel materials could create the micro-scale objects.

Here, we report 3D printable gel phantoms including inter crosslinking network (ICN) that can reversibly switch between transparent and opaque states. Although the aim of this study is to develop the patient-specific phantoms that are equivalent to human tissues containing a lot of water, accidentally we found that ICN gels have a phase transition due to changing water content. ICN gels with an ordered structure were synthesized by the copolymerization of the monomer, *N,N*-dimethylacrylamide (DMAAm), the rigid-rod polymer, hydroxypropyl cellulose (HPC, the viscosity = 150–400 cP) and the crosslinker, 2-(2-methacryloyloxyethoxy)ethyl isocyanate (Kareznz MOI-EG). Chemicals as the ultraviolet (UV) initiator are depending on the wavelength of laser source in the process of how we fabricate ICN gels. UV Initiator was added to create the radicals in the ICN gels because of use of UV instead of radiation. As reported earlier (Hidemitsu et al. 2013; Go et al. 2012), high ductility of ICN gels with high water content was derived from a rare type of network which has crosslinking structure only between the different types of polymer, pDMAAm and HPC. After fabrication the ICN gels, ICN gels were dipping in the 2nd gel solution including the UV initiator. The initiator of 2nd gel solution create the free radicals, which induce the polymerization led to opacity in the ICN gel phantom, instead of the free radicals resulting from water radiolysis.

## 2 Materials and methods

### 2.1 Materials

Liquid of DMAAm were obtained from Tokyo Chemical Industry Co., Ltd., Japan and used as monomer. Powder of the HPC, *N,N'*-methylenebisacrylamide (MBAA) and 2-oxoglutaric acid ( $\alpha$ -keto) were obtained from Wako Pure Chemical Industries Ltd., Japan and used as rigid polymer, crosslinking agent and water-soluble photo initiators, respectively. The Kareznz MOI-EG were provided by Showa Denko K.K., Japan and used as crosslinking agent. 2-Hydroxy-1-[4-[4-(2-hydroxy-2-methyl-propionyl)-benzyl]-phenyl]-2-methylpropan-1-one (Irgacure 127) and 5-benzoyl-4-hydroxy-2-methoxybenzenesulfonic acid (Kemisorp 11S) were purchased from BASF Japan and Sigma-Aldrich Co., Ltd., respectively and used as photo initiator and UV absorber for 3D printing, respectively. All the above reagents were used without further purification.

### 2.2 Fabrication of ICN phantoms by mold technique

The ICN gel phantoms are synthesized via a two-step sequential free-radical polymerization process. At first, ICN gels were synthesized from 1st aqueous solution of 1 M DMAAm containing 0.5 mol% rigid polymer, HPC, 0.1 mol% crosslinking agent, Kareznz MOI-EG, and 0.008 mol% initiator, Irgacure 127, in a reaction mold consisting of a pair of glass plates with spacing. The synthesized ICN gels were immersed in 2nd gel solution for 2 days to be in equilibrium swollen state, and thereafter the swollen ICN gels were irradiated with a UV LEDs of 12.4 mW/cm<sup>2</sup> with a peak emission wavelength of 375 nm in the customized incubator set at 30 °C. In the case of low concentration of MBAA, the crosslinking agent of 2nd gels, the opacity of ICN gel phantoms cannot be derived from UV irradiation. That is reason why the ratio of MBAA to DMAAm in the 2nd gel solution shown in Table 1 is much higher than the ratio of Kareznz MOI-EG to DMAAm in the synthesis of ICN gels.

All units of numbers in Table 1 are mol% to DMAAm 1 M of each solution.

### 2.3 Method of characterization

The transmittance spectra of the ICN gels was recorded with UV-2550 Shimadzu spectrometer. The opacity was characterized at the transmittance at the wavelength of 550 nm.

#### 2.3.1 3D fabrication of ICN Gel phantom

We have fabricated the ICN gel phantom (3DP46) using the customized 3D printer manufactured by D-lightmatter Co., Ltd (2019). The ICN gels have been discharged with the dispenser to the stage of the 3D printer. This 3D printer has stage of 300 × 300 × 200 mm and a high resolution along the X and Y axis 500  $\mu$ m. The linear irradiation type of UV LED unit, LC-L5G Hamamatsu Co., Ltd., with wavelength of 365 nm and maximum UV irradiance 6 W/cm<sup>2</sup> was used for polymerization in the fabrication process. The synthesis ratio of the crosslinkers, monomer, initiator and solvent has been kept same as Mold46. These are used with critical optimization of composition. The reason for using Irgacure 127 is because it was observed that, during 3D printing,  $\alpha$ -keto created more scattering of UV laser, forming somewhat broad structure, while choosing Irgacure 127, it was possible to control the laser scattering easily. Additionally, 0.5 mol% UV absorber, Kemisorb11S has been used to control gelation range and prevent further scattering of UV light for making fine structures. The ICN

**Table 1** Composition ICN gel phantom

Sample	1st gel solution					2nd gel solution		
	HPC	Karenz MOI-EG	Irgacure 127	Water	Kemisorb 11S	MBAA	$\alpha$ -keto	Water
Mold 10	0.6	0.6	0.008	371	NA	10	1.0	11,700
Mold 23	0.6	0.6	0.008	371	NA	23	1.0	11,700
Mold 46	0.6	0.6	0.008	371	NA	46	1.0	11,700
3DP 46	0.6	0.6	0.008	371	0.5	46	1.0	11,700

gels was kept in the glove box except during preparation of pre-gel solution and the pre-gel solution has been kept in a brown plastic seal bottle before transferring them to the dispenser of 3D printer. The 3D printed ICN gels were immersed in 2nd gel solution for 2 days to be in equilibrium swollen state. After swelling, the ICN gel phantom was set on the turntable in the UV chamber to realize homogeneous distributions of UV irradiation, and irradiated for 7 min in the customized incubator.

### 3 Results and discussions

#### 3.1 Opacity of ICN phantoms

Three ICN phantoms by using a mold technique with different molar ratios of MBAA to DMAAm at 10:1.0 (Mold 10), 23:1.0 (Mold 23) and 46:1.0 (Mold 46) in 2nd gel solution were synthesized to evaluate the performance of gel phantom. Figure 1 displays the pictures of ICN phantoms at each UV exposure time. As is shown, all samples gradually turned white; that is, the polymerization of monomers of 2nd gel solution in 1st ICN gels proceeded with increases in the time of UV light irradiation. It is noted that the radical from UV initiator in the ICN phantoms initiate the polymerization similar to conventional gel dosimeter (Kiyofumi et al. 2007; Shinichiro 2013; Baldock et al. 2010).

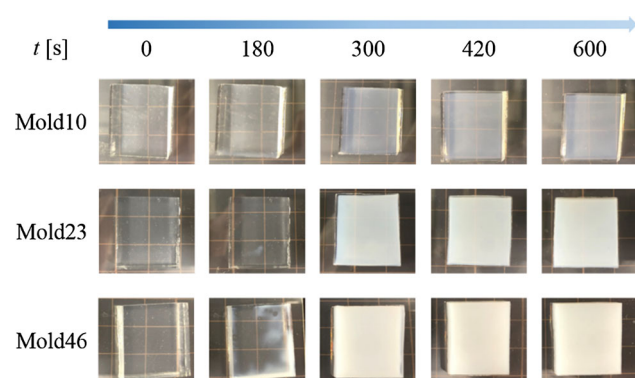


**Fig. 1** The change in appearance of ICN gels (Mold10, Mold23 and Mold46) at each UV exposure time (0, 180, 300, 420 and 600 s)

To quantitatively evaluate the opacity of ICN phantoms, the degree of opacity ( $T$ , %) at the wavelength of 550 nm observed with UV-2550 was nondimensionalized by the initial degree of opacity ( $T_0$ , %). The nondimensionalized value ( $T/T_0$ , -) of each gel decrease exponentially with increases in the time of UV irradiation in Fig. 2. If it is simply assumed that the opacity of phantoms follow chemical reaction rate theory, the nondimensionalized value ( $T/T_0$ , -) is analytically obtained by the following formula (Eisenberg and Donald 1996):

$$\frac{T}{T_0} = e^{-\Gamma t} + C, \tag{1}$$

where  $\Gamma$  represents the rate of chemical reaction,  $t$  represents the time of UV light irradiation and  $C$  represents the constant number. Based on the least-squares fitting method for formula (1),  $\Gamma$  and  $C$  of each gel in Table 2 was obtained, and the approximate curves of each gel were drawn in Fig. 2. As shown Fig. 2,  $T/T_0$  decreases at a decreasing rate with increases in time  $t$ , and tends to the value  $C$ . The final values of opacity of ICN phantoms  $C$  depends on the concentration of MBAA owing to creating the clusters containing much MBAA, which scatter

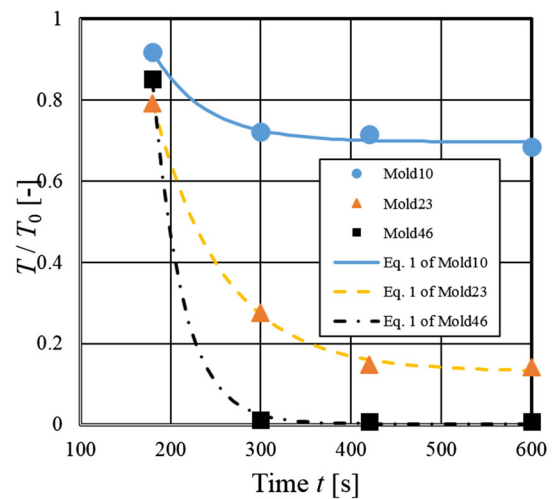


**Fig. 2** The change in opacity of ICN gels (Mold10, Mold23 and Mold46) after UV-treatment, recorded with UV-2550 Shimadzu spectrometer at 550 nm, decrease exponentially with increases in the time of UV treatment. The plots are experiment value, and the approximate curves are calculated by formula (1)

**Table 2** The rate of chemical reaction  $\Gamma$  and the constant value  $C$  in formula (1) for each ICN phantom

Sample	$\Gamma$ (1/s) [ $1/\Gamma$ (s)]	$C$ (-)
Mold 10	0.017 [60]	0.69
Mold 23	0.013 [80]	0.13
Mold 46	0.030 [33]	0.0019

visible light. These clusters were spatially fixed in the 1st gel network. On the contrary, since the rate of chemical reaction  $\Gamma$  of Mold23 is slowest of three samples,  $\Gamma$  does not depend on the concentration of MBAA simply.

Furthermore, the UV irradiated ICN phantoms turn to transparent after deswelling. It was found that the transparent-opaque transition is reversible as shown in Fig. 3. This phenomena demonstrates that the MBAA clusters were homogenized by shrinking of gel network, but the positional information of the clusters was spatially saved in the dry state.

### 3.2 Fabrication of ICN gel phantom

We have fabricated the ICN gel phantom (3DP46) using the customized 3D printer with the fluid-dispensing head. The publicly available 3D data of a right index finger under

the license CC-BY SA 2.1JP (BodyParts3D/Anatomography 2019) was used for the development of the life-sized ICN gel phantom (Fig. 4a). The 1st gel solution of 3DP46, whose synthesis ratio is suitable for the customized 3D printer, was similar ratio to Mold46 because Mold46 was the most sensitive for UV irradiation of the three ICN gels. The finger shape of 1st ICN gel was replicated (Fig. 4b). This is the first ever report of highly stable ICN network gels that can also be 3D printable by optical fabrication of stereolithography using a dispenser up to micro resolution. In order to add UV sensitivity to the 3D printed ICN gels instead of dose sensitivity, the 3D printed ICN gel were immersed in 2nd gel solution, including a photo initiator, to be in equilibrium swollen state: ICN gel phantom (Fig. 4c). The swollen state was about 3.5 times as heavy as before. After UV irradiation for 7 min, the ICN gel phantom turned to opaque from transparent due to photo polymerization (Fig. 4d). In the cross section of ICN gel phantom as shown Fig. 4e represented the inhomogeneous distributions of actual UV irradiation. For example, enough UV light for polymerization did not pass through at the center of the cross section, and so the center kept transparent after UV irradiation.

**Fig. 3** Influence of water content on the transparent-opaque transition of ICN gels

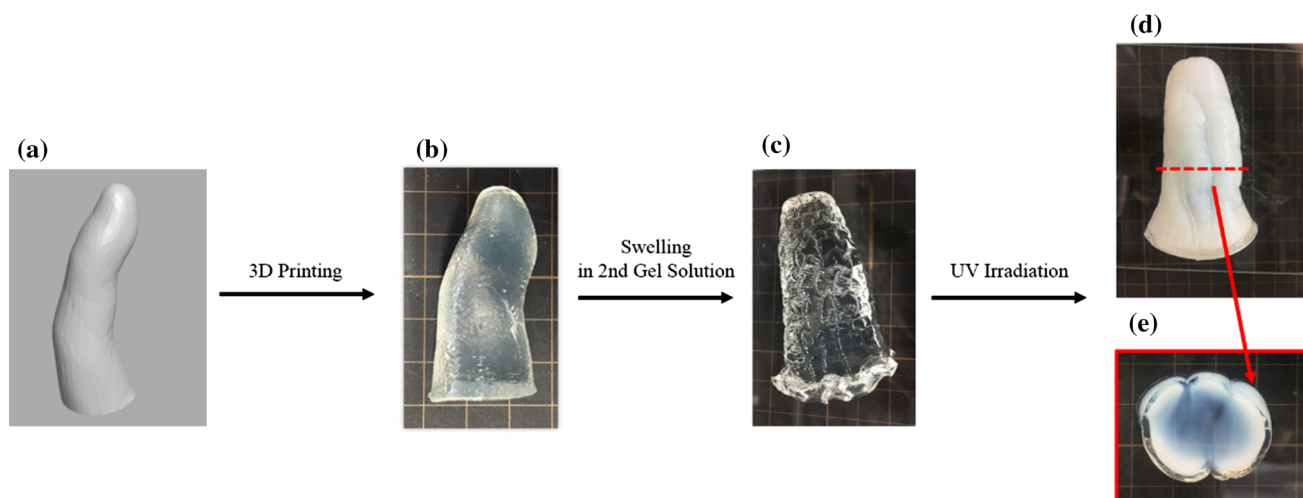
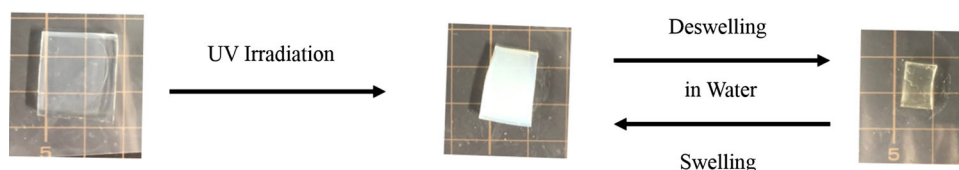


**Fig. 4** Process of fabrication of ICN gel phantom. **a** 3D modeling of a right index finger. **b** 3D printed ICN gel. **c** 3D printed ICN gel swollen with 2nd gel solution: ICN gel phantom. **d** ICN gel phantom after UV irradiation. **e** Cross section of **d**



## 4 Conclusions

In the current study, the double network gels having ICN:ICN gel were used as the gel phantom, which has sensitivity for UV irradiation. The opacity of three ICN phantoms with the molar ratios of MBAA to DMAAm at 10:1.0, 23:1.0 and 46:1.0 in the 2nd gel solution were observed with UV-2550 after UV irradiation. With the decreasing molar fraction, the final opacity become higher, but the rate of polymerization may not be estimated by the molar fraction simply. Besides, we observed that photo polymerized ICN phantom can reversibly switch between transparent and opaque states with changing water content in the network.

We confirmed that ICN gel was fabricated with the customized 3D printer with a high resolution 500  $\mu\text{m}$  as the pre-finger-shaped phantom. For the chemical composition specialized in 3D printing process, we considered photo initiators and UV absorbers. The immersion into 2nd gel solution enable us to add sensitivity for UV light to the 3D printed ICN gel. The cross section of swollen 3D printed ICN gel after UV irradiation showed the distribution of UV light after UV irradiation similar to gel dosimeter. We expect that the 3D printer specialized gel materials and ICN gels are feasible for practical fabrication method of 3D gel phantom.

**Acknowledgements** The authors would like to thank K. Takamatsu for technical assistance with the fabrication of ICN gels.

**Funding** This work was funded in part by JSPS KAKENHI Grant number JP17H01224, JSPS KAKENHI Grant number JP18H05471, JST COI Grant number JPMJCE1314, JST -OPERA Program Grant number JPMJOP1844, JST -OPERA Program Grant number JPMJOP1614, and the Cabinet Office (CAO), New Energy and Industrial Technology Development Organization (1st and 2nd Cross-ministerial Strategic Innovation Promotion Program (SIP)), “An intelligent knowledge processing infrastructure, integrating physical and virtual domains” (funding agency: NEDO).

## Compliance with ethical standards

**Conflict of interest** The authors declare no conflicts of interest.

**Open Access** This article is distributed under the terms of the Creative Commons Attribution 4.0 International License (<http://creativecommons.org/licenses/by/4.0/>), which permits unrestricted use, distribution, and reproduction in any medium, provided you give appropriate credit to the original author(s) and the source, provide a link to the Creative Commons license, and indicate if changes were made.

## References

D-lightmatter Co., Ltd. (2019). <http://d-lightmatter.com/>. Accessed 27 June 2019

- Baldock C, De DY, Doran S, Ibbott G (2010) Topical review: polymer gel dosimetry. *Phys Med Biol* 55(5):R1–R63. <https://doi.org/10.1088/0031-9155/55/5/R01>
- BodyParts3D/Anatomography (2019). <https://lifesciencedb.jp/bp3d/>. Accessed 27 June 2019
- Eisenberg DS, Donald M (1996) *Physical chemistry with applications to the life sciences*. Baifukan, Tokyo
- Elter A, Dorsch S, Mann P et al (2019) Compatibility of 3D printing materials and printing techniques with PAGAT gel dosimetry. *Phys Med Biol* 64:04NT02. <https://doi.org/10.1088/1361-6560/aafef0>
- Etsuo K (2017) Radiotherapy updates applications of high precision radiotherapy and intensity modulated radiotherapy. *Radioisotopes*. <https://doi.org/10.3769/radioisotopes.66.201>
- Fabian A, Tian Q, Andrew M et al (2016) Soft 3D-printed phantom of the human kidney with collecting system. *Ann Biomed Eng* 45(4):963–972. <https://doi.org/10.1007/s10439-016-1757-5>
- Forte Antonio E, Stefano G, Francesco M (2016) A composite hydrogel for brain tissue phantoms. *Mater Des* 112:227–238. <https://doi.org/10.1016/j.matdes.2016.09.063>
- Go T, Ruri H, Hidemitsu F (2012) Ultrahigh ductile gels having inter-crosslinking network (ICN) structure. *J Solid Mech Mater Eng* 6(2):169–177. <https://doi.org/10.1299/jmmp.6.169>
- Hidemitsu F, Ruri H, Go T et al (2013) Smart hydrogels developed with inter-crosslinking network (ICN) structure. *J Solid Mech Mater Eng* 7(2):245–250. <https://doi.org/10.1299/jmmp.7.245>
- Kiyofumi H, Hiroki M, Munenori Y et al (2007) Comparison evaluation of polymer gel with a water phantom. *Jpn J Med Phys* 26:4. [https://doi.org/10.11323/jjmp2000.26.4\\_199](https://doi.org/10.11323/jjmp2000.26.4_199)
- Kumkum A, Naofumi N, Masaru K et al (2018) Extremely soft, conductive, and transparent ionic gels by 3D optical printing. *Macromol Chem Phys* 219:1800216. <https://doi.org/10.1002/macp.201800216>
- Leonard HL, Tiantian Y, John MW (2018) A polymer-gel eye-phantom for 3D fluorescent imaging of millimetre radiation beams. *Polymers* 10:1195. <https://doi.org/10.3390/polym10111195>
- Pantelis E, Moutsatsos A, Antypas C et al (2018) On the total system error of a robotic radiosurgery system: phantom measurements, clinical evaluation and long-term analysis. *Phys Med Biol* 63:165015. <https://doi.org/10.1088/1361-6560/aad516>
- Shiblee MDNI, Kumkum A, Masaru K et al (2019) 4D printing of shape-memory hydrogels for soft-robotic functions. *Adv Mater Technol*. <https://doi.org/10.1002/admt.201900071>
- Shinichiro H (2013) Verification of 3D dose distribution using polymer gel dosimeter. *Jpn J Med Phys* 32(3):125–129. [https://doi.org/10.11323/jjmp.32.3\\_125](https://doi.org/10.11323/jjmp.32.3_125)
- Takeshi K, Hidetoshi S, Takayoshi N et al (2017) Three-dimensional printer-generated patient-specific phantom for artificial in vivo dosimetry in radiotherapy quality assurance. *Phys Med* 44:205–211. <https://doi.org/10.1016/j.ejmp.2017.10.005>
- Wagter CD (2004) The ideal dosimeter for intensity modulated radiation therapy (IMRT): what is required? *J Phys Conf Ser* 3:4. <https://doi.org/10.1088/1742-6596/3/1/002>
- Yuichiro N (2004) Scene of the intensity modulated radiation therapy (IMRT): all for patient!! *Jpn J Radiol Technol* 61:5
- Yuichiro N, Kazuo H, Takayuki S et al (2002) Dosimetric verification in intensity modulated radiation therapy. *Jpn J Radiol Technol* 58:6

**Publisher's Note** Springer Nature remains neutral with regard to jurisdictional claims in published maps and institutional affiliations.